



Contents lists available at ScienceDirect

Biochemical and Biophysical Research Communications

journal homepage: [www.elsevier.com/locate/ybbrc](http://www.elsevier.com/locate/ybbrc)



# EML4-ALK induces epithelial–mesenchymal transition consistent with cancer stem cell properties in H1299 non-small cell lung cancer cells



Fuchun Guo, Xiaoke Liu, Qin Qing, Yaxiong Sang, Chengjun Feng, Xiaoyu Li, Li Jiang, Pei Su, Yongsheng Wang\*

Department of Thoracic Oncology, Cancer Center, State Key Laboratory of Biotherapy/Collaborative Innovation Center of Biotherapy, West China Hospital, Sichuan University, Chengdu, Sichuan, PR China

## ARTICLE INFO

### Article history:

Received 12 February 2015

Available online 28 February 2015

### Keywords:

EML4-ALK

EMT

Cancer stem cell

ERK1/2

## ABSTRACT

The echinoderm microtubule-associated protein-like 4 (EML4) – anaplastic lymphoma kinase (ALK) fusion gene has been identified as a driver mutation in non-small-cell lung cancer (NSCLC). However, the role of EML4-ALK in malignant transformation is not entirely clear. Here, for the first time, we showed that H1299 NSCLC cells stably expressing EML4-ALK acquire EMT phenotype, associated with enhanced invasive migration and increased expression of EMT-inducing transcription factors. H1299-EML4-ALK cells also displayed cancer stem cell-like properties with a concomitant up-regulation of CD133 and enhanced ability of mammospheres formation. Moreover, we found that inhibition of ERK1/2 reversed EMT induced by EML4-ALK in H1299 cells. Taken together, these results suggested that EML4-ALK induced ERK activation is mechanistically associated with EMT phenotype. Thus, inhibition of ERK signaling pathway could be a potential strategy in treatment of NSCLC patients with EML4-ALK translocation.

© 2015 Elsevier Inc. All rights reserved.

## 1. Introduction

Echinoderm microtubule-associated protein–like 4-anaplastic lymphoma kinase (EML4-ALK), resulting from the chromosome inversion inv(2) (p21; p23), was identified as a transforming gene in non–small cell lung cancer (NSCLC) [1]. The incidence of EML4-ALK NSCLC is approximately 5%, equivalent to over 70,000 patients diagnosed annually worldwide [2]. EML4-ALK translocations, with histological features of acinar pattern or signet-ring cell, tends to present in young patients and those who possess wild-type EGFR and KRAS genes [2–4]. Clinical trials have shown a high rate of responses of ALK-rearranged tumors to the inhibition of the ALK activity by crizotinib, a specific ALK inhibitor [5]. Unfortunately, not all patients with ALK<sup>+</sup> non–small cell lung cancer (NSCLC) benefit from ALK inhibition [5] and acquired drug resistance inevitably

develops in patients who initially do respond [6]. Therefore, more study on the role of EML4-ALK is required to improve the treatment.

Acquisition of invasive properties is critical in the tumor progression [7]. Within cancer of epithelial origin, acquisition of invasiveness requires a dramatic morphological alteration which termed epithelial–mesenchymal transition (EMT), wherein cancer cells in primary tumor lose their epithelial characteristics of cell polarity and switch to a motile fibroblastoid or mesenchymal phenotype. Epithelial cells lose cell–cell adhesions mediated by E-cadherin (one of the epithelial markers) repression is considered to be a crucial step in EMT [8]. Intensive studies revealed that down-regulation of E-cadherin and increased expression of mesenchymal markers (e.g., vimentin and fibronectin) is triggered by an interplay of intracellular and extracellular signals [9]. The activation of signaling pathways also leads to the activation of transcriptional factors such as snail and slug, which change patterns of gene expression underlying EMT [10].

In addition to accompanying behavioral changes such as enhanced mobility and invasiveness, increasing evidences suggests that cells undergo Epithelial-mesenchymal transition gain stem

\* Corresponding author.

E-mail addresses: [liuxk57@163.com](mailto:liuxk57@163.com) (X. Liu), [qinqingscu@126.com](mailto:qinqingscu@126.com) (Q. Qing), [yaxionsang@gmail.com](mailto:yaxionsang@gmail.com) (Y. Sang), [leymj@163.com](mailto:leymj@163.com) (C. Feng), [lixiaoyu2012huaxi@163.com](mailto:lixiaoyu2012huaxi@163.com) (X. Li), [summer.jl06@foxmail.com](mailto:summer.jl06@foxmail.com) (L. Jiang), [keyanxiaozhu@163.com](mailto:keyanxiaozhu@163.com) (P. Su), [wangys@scu.edu.cn](mailto:wangys@scu.edu.cn) (Y. Wang).

cell-like phenotype, thus giving rise to cancer stem cells (CSCs) [11,12]. Mani, S. A. and colleagues have demonstrated that both overexpression of the EMT-inducing transcription factors Twist1 or Snai1 and treatment with TGF $\beta$  increase the number of stem cells, consistent with the increased expression of cell surface antigenic profiles and enhanced ability of mammospheres formation in mammary epithelial cells. This property conferred by EMT not only enables the carcinoma cells to migrate to metastatic dissemination, but also qualify them with properties of stemness, enabled to tumorigenesis and proliferation. Thus, owing to the clinical importance of the EMT-induced processes, treatments eliciting a mesenchymal–epithelial transition (MET) could be an attractive therapeutic approach on tumor.

Previous observations have showed EML4-ALK as a transforming fusion gene in non-small cell lung cancer (NSCLC) [1,13], however, the role of EML4-ALK in malignant transformation such as EMT and cancer stem cell-like characteristics is not clear. The aim of the this study was to obtain additional insights into the role of EML4-ALK in NSCLC. Using EML4-ALK stably expressing H1299 cells, we investigated the effects of EML4-ALK on malignant biological behavior of NSCLC.

## 2. Materials and methods

### 2.1. Cell culture and reagents

The human non-small cell lung cancer cell line H1299 were obtained from American Type culture Collection (ATCC) and cultured in RPMI-1640 Medium containing 10% fetal bovine serum with 1% penicillin/streptomycin (SIGMA, USA) under a incubator humidified atmosphere of 5% CO $_2$  at 37 °C. FR180204, crizotinib and S31-201 were obtained from selleck.

### 2.2. Cell transfection

Human EML4-ALK V1 expression vector with puromycin-resistance gene was kindly provided by Dr Hiroyuki Mano (Jichi Medical University, Japan). Stable transfectants of H1299 cells with EML4-ALK were isolated after selection with puromycin (Invitrogen, USA) at 0.8  $\mu$ g/ml using lentivirus system, and further screened with western blot analysis for EML4-ALK expression. H1299 cells transfected with control vector was used as a negative control.

### 2.3. Western blotting

Cells were washed three times with ice-cold PBS and then lysed in RIPA lysis buffer (Beyotime, China) on ice. The protein concentration of cell lysates was determined by bicinchoninic acid (BCA) protein assay. Equal amounts of protein were subjected to SDS-PAGE on a 8% or 10% gel and then transferred onto polyvinylidenedifluoride (PVDF) membranes (Millipore, USA). Membranes were blocked with 5% nonfat dried milk in TBST (10 mM Tris, pH 7.4/150 mM NaCl and 0.1% Tween-20) for 1 h at room temperature before incubation with primary antibody overnight at 4 °C. The primary antibodies used in this study were as follows: mouse antibody to ALK, rabbit antibody to human phosphorylated ALK (pY1608), Ecadherin, phosphorylated STAT3 (pTyr705) and STAT3 were obtained from abcam, those to phosphorylated extracellular signal-regulated kinase 1/2 (ERK1/2) (pThr202/Tyr204), to ERK1/2 were from cell signaling Technology; those to  $\beta$ -actin from santa cruz biotechnology. All antibodies were used at a 1:1000 dilution. The membrane were washed with TBST before reacted with HRP-conjugated anti-rabbit or mouse IgG (Beyotime, China) for 1 h at room temperature. After washing with

TBST and Tris-buffered saline, immune complexes were visualized by the enhanced chemiluminescence (ECL) detection.

### 2.4. RNA extraction and analysis by quantitative real-time PCR

Total RNA was extracted and purified using RNA simple Total RNA Kit (TIANGEN BIOTECH, China) according to the manufacturer's instructions. The RNA samples were reverse-transcribed into cDNA with the PrimeScript<sup>TM</sup> RT reagent Kit (TAKARA, Japan). Quantitative real-time PCR was conducted with Bio-rad CFX manager and SsoAdvanced SYBR Green Supermix (Bio-rad, USA) as the detection reagent. All samples were analyzed in triplicate for each primer set. The primer sequences of PCR were as follows: hSox2, sense 5'- AGAACCCCAAGATGCACAAC -3' and antisense 5'- CGG GGCCGGTATTATAATC -3'; hNanog, sense 5'- TGAACCTCAGCTACA AACAGGTG-3' and antisense 5'- AACTGCATGCAGGACTGCAGAG -3'; hOct3/4, sense 5'- CTTGCTGCAGAACTGGGTGGAGGAA -3' and antisense 5'- CTGCAGTGTGGGTTTCGGGCA-3'; hTGF- $\beta$ 1, sense 5'- C TAATGGTGGAAACCCACAACG -3' and antisense 5'- TATGCCAGGA ATTGTGCTG -3'; hGAPDH, sense 5'- GAAGGTGAAGGTCCGAGT-3' and antisense 5'- GAAGATGGTGATGGGATTTC-3'. Primer sets for hEcad, hFN1, hNcad, hVim, hSnail and hSlug were as described [11]. RT-PCR amplification was performed 40 cycles with DNA denaturation at 95 °C for 5 s and annealing/extension at 60 °C for 20 s. Target gene expression was quantified with the relative quantification method.

### 2.5. TGF- $\beta$ ELISA assay

The amount of total TGF- $\beta$ 1 in the media was quantified by ELISA kit (DAKEWE, China). The assay was performed according to the manufacturer's instructions and measured with Multiskan MK3 microplate spectrophotometer (Thermo scientific, Finland).

### 2.6. Wound healing assay

Briefly, Cells were grown in a confluent monolayer in 6-well plates and then serum-starved overnight. A wound was created in the cell layer by scratching the plate with a plastic yellow pipette tip. After washing with media, the cells were incubated in growth medium with or without inhibitors for 16 h and photographed under a microscope. The migration distance was measured, Each assay were repeated at least three times.

### 2.7. Cell migration assay

Cells were serum starved for 24 h prior to use.  $5 \times 10^4$  cells per well in 100  $\mu$ l serum-free media were added in the upper chamber of a 8  $\mu$ m pore size micropore polycarbonate membrane transwell filter (Millipore, USA), which were placed in 24-well plate with 600  $\mu$ l RPMI 1640 containing 10% FBS as chemo-attractant in the lower chamber. Cells were incubated at 37 °C in 5% CO $_2$  for 4 h. Then, the upper surface of filter was carefully removed with a cotton swab, insert membranes were fixed with cold methanol for 10 min, stained with 0.1% crystal violet for 20 min. Finally, migrated cells were photographed and counted under a light microscope (5 fields per chamber).

### 2.8. Cell invasion assay

Polycarbonate membranes of chambers were coated with Matrigel (BD Biosciences, USA) on the upper surface.  $2 \times 10^4$  Cells starved from serum for 24 h were resuspended in serum-free RPMI1640 and added to the upper chamber in 0.1 ml of serum-free medium. RPMI1640 medium supplemented with 10% FBS

was added to the lower chamber as chemo-attractant. The cells were incubated for 16 h in 5% CO<sub>2</sub> at 37 °C. Non-invading cells were removed with a cotton-tipped swab from the top of the Matrigel. The invasive cells were examined by bright field microscopy and counted from five randomly chosen fields.

## 2.9. Flow cytometry

Cells were collected and dissociated as single cells, washed with 0.1% bovine serum albumin in PBS (PBSA) and incubated with appropriate dilution of APC-conjugated anti-human CD133 antibody or control antibody (BD Pharmingen, USA). After incubating for 30 min, cells were washed and resuspended in PBS, then performed on a BD Biosciences FACSCalibur cytometer. Data were analyzed using FlowJo.

## 2.10. Sphere formation assay

Mammosphere formation assay was done in ultra-low attachment 96-well plates (Corning) at a density of 1000 viable cells/mL and grown in a serum-free Dulbecco's modified Eagle medium/F12 (Sigma, USA) supplemented with B27 (Invitrogen, USA), 20 ng/mL of EGF and 20 ng/mL of bFGF (Invitrogen, USA), and 4 mg/mL of heparin (Sigma, USA). Cells were allowed to form spheroids for 10 days, and the numbers of spheres were counted in microscope.

## 2.11. Statistical analysis

All of the statistical analyses were performed using the Graphpad Prism software program. Data analysis for multiple groups was carried out using the one-way ANOVA Tukey test. And data analysis for two groups was carried out using t test. All data were summarized and presented as means  $\pm$  SD,  $P < 0.05$  were considered to indicate statistically significant differences.

# 3. Results

## 3.1. Expression of EML4-ALK induced epithelial–mesenchymal transition in H1299 non-small cell lung cancer cells

To demonstrate the role of EML4-ALK in aggressiveness of lung cancer cells, we generated stable cell lines (H1299-EML4-ALK) from H1299 human NSCLC cells using lentiviral infection system with plasmid vectors encoding EML4-ALK cDNA. An empty vector-transfected control (H1299-Ctrl) was produced simultaneously. Interestingly, we observed morphologic differences using a light microscope. Expression of EML4-ALK induced spindle-like, elongated fibroblastic appearance in H1299 cells which normally exhibit a flat epitheloid morphology, suggesting that EMT-like changes might have occurred (Fig. 1A). To confirm the induction of EMT in H1299-EML4-ALK cells, we analyzed the expression of epithelial and mesenchymal markers using western blots and quantitative real-time PCR. As shown in Fig. 1B, in addition to the EML4-ALK activated signaling pathway such as ERK and STAT3, we demonstrated that H1299-EML4-ALK cells, compared with H1299 Ctrl cells, displayed a remarkable ablation of the protein expression of epithelial marker E-cadherin. Consistent with this finding, compared with the H1299 Ctrl cells, mRNA expression of E-cadherin were drastically reduced (~3-fold) and mesenchymal markers such as fibronectin 1 was increased in H1299-EML4-ALK cells (~1.5-fold), but the expression of other two mesenchymal markers vimentin and Ncadherin showed no significant difference (Fig. 1C). In addition, the levels of several EMT inducing factors were increased, such as snail (~2-fold) and slug (~9-fold) (Fig. 1D). Taken

together, these observations indicated that EML4-ALK was able to induce EMT in H1299 non-small cell lung cancer cells.

## Expression of EML4-ALK promotes invasion and migration in vitro

The invasive and migratory potential were considered functional hallmarks of EMT in tumor cells. Therefore, we detected the changes of invasive and migratory ability of H1299 cells expressing EML4-ALK by transwell invasion and migration assay. The results revealed that, compared with H1299 Ctrl cells, the invasive H1299-EML4-ALK cells that had spread through the filter and adhered the underside significantly increased (~10-fold), as well as the migrated cells (~6-fold) (Fig. 2A). Further, we analyzed the protein levels of MMP-2 and -9, two crucial proteins involved in cancer cell metastasis. The Western blotting results showed that the protein levels of MMP-2 and MMP-9 were significantly increased in cells of EML4-ALK expression compared with control cells (Fig. 2B). EML4-ALK induced changes in migration were further confirmed by wound-healing migration assay (Fig. 2C). Our findings suggested that expression of EML4-ALK in H1299 cells attributed to increased expression of MMP2 and MMP9, modulating invasive migration during EMT.

## 3.3. Expression of EML4-ALK enhanced sphere formation and stem cell-like properties in H1299 cells

Recent evidence suggests that EMT not only plays a critical role in tumor metastasis but cells undergo EMT also gain stem cell-like properties, giving rise to cancer stem cells (CSCs). Therefore, we detected the capacity of CSC in this study. First, flow cytometry analysis showed an increased population of CD133<sup>+</sup> cells in H1299-EML4-ALK clones. About 3% of the cells were determined as CD133<sup>+</sup> in H1299-EML4-ALK cells, whereas CD133<sup>+</sup> cells were nearly undetectable in H1299-Ctrl cells (Fig. 3A). Second, Sphere formation was an important measurement used to define malignant cancers and cancer stem-like cells. Accordingly, H1299-EML4-ALK cells displayed significantly enhanced ability to form mammosphere relative to H1299-Ctrl cells. As shown in Fig. 3B, the number of mammospheres of H1299-EML4-ALK cells increased about 5-fold compared to H1299-Ctrl cells. To further discover the genes regulating the stem cell properties of H1299-EML4-ALK cells, we performed real time RT-PCR analysis of stem cell-specific genes. The mRNA level of selected markers, Sox2, Oct3/4 and Nanog, were also increased in H1299-EML4-ALK cells. The elevated stem cell specific markers suggested that H1299-EML4-ALK might have undergone certain process, shifting cellular properties toward stem cell or cancer stem cell.

## 3.4. ERK1/2 inhibition reverse EML4-ALK induced epithelial–mesenchymal transition in H1299 cells

Because TGF- $\beta$ 1 has been shown to play an important role in Epithelial–Mesenchymal Transition, we explored whether expression of EML4-ALK in H1299 cells increased TGF- $\beta$ 1 production. The mRNA expression and secretion of TGF- $\beta$ 1 were detected by quantitative real-time PCR and elisa respectively. however, there was no significant difference between EML4-ALK expressing H1299 cells and control cells (Fig. 4A). We next probed the connection between EML4-ALK induced signaling pathways and EMT. To determine the role of intracellular activation of ERK1/2, STAT3 in this action, we evaluated the effects with chemical inhibitors. We found that morphologic changes induced by EML4-ALK were reversed by inhibition of ERK1/2 and ALK, but not STAT3 (Fig. 4B). Consistent with this observation, We showed that the selected inhibitor FR180204, effectively inhibiting ERK1/2 phosphorylation at

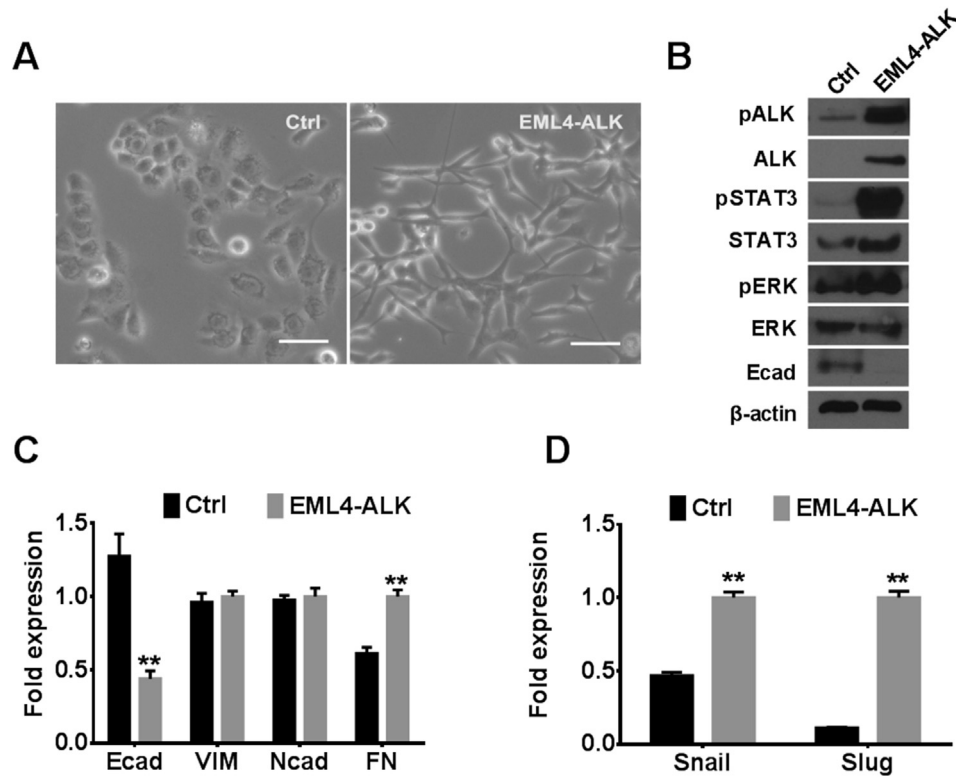


**Fig. 1.** H1299-EML4-ALK show an EMT phenotype. (A) Morphology of H1299-Ctrl and H1299-EML4-ALK cells. Scale bars: 50  $\mu$ m. (B) The expression of E-cadherin, ALK, pALK, STAT3, pSTAT3, ERK1/2, and pERK1/2 of H1299-Ctrl and H1299-EML4-ALK cells were examined by western blotting.  $\beta$ -actin serves as the loading control. (C,D) Quantitative RT-PCR was used to quantify E-cadherin, Vimentin, N-cadherin, fibronectin, snail and slug mRNA expression in H1299-Ctrl and H1299-EML4-ALK cells. \* $P < 0.05$ ; \*\* $P < 0.01$ .

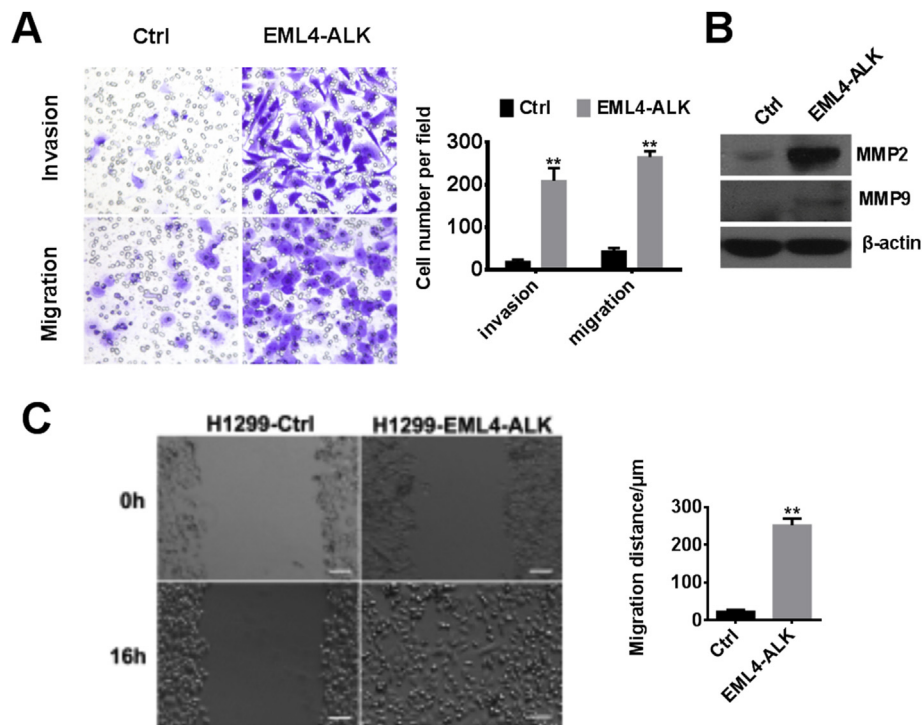


**Fig. 2.** H1299-EML4-ALK cells have enhanced invasive and migratory potential. (A) Transwell migration and invasion assays of H1299-Ctrl and H1299-EML4-ALK cells. The mean data of five fields in the lower side were counted. Data represent means  $\pm$  SEM of three independent experiments. \* $P < 0.05$ ; \*\* $P < 0.01$ ; (B) Expression of MMP-2 and MMP-9 were detected by Western blot.  $\beta$ -actin loading control is also shown. (C) Motility of H1299-Ctrl and H1299-EML4-ALK cells as measured by wound-healing assay. The distance of migration was calculated from the mean of seven wound widths with S.D. \*\* $P < 0.01$ . Scale bars: 100  $\mu$ m.



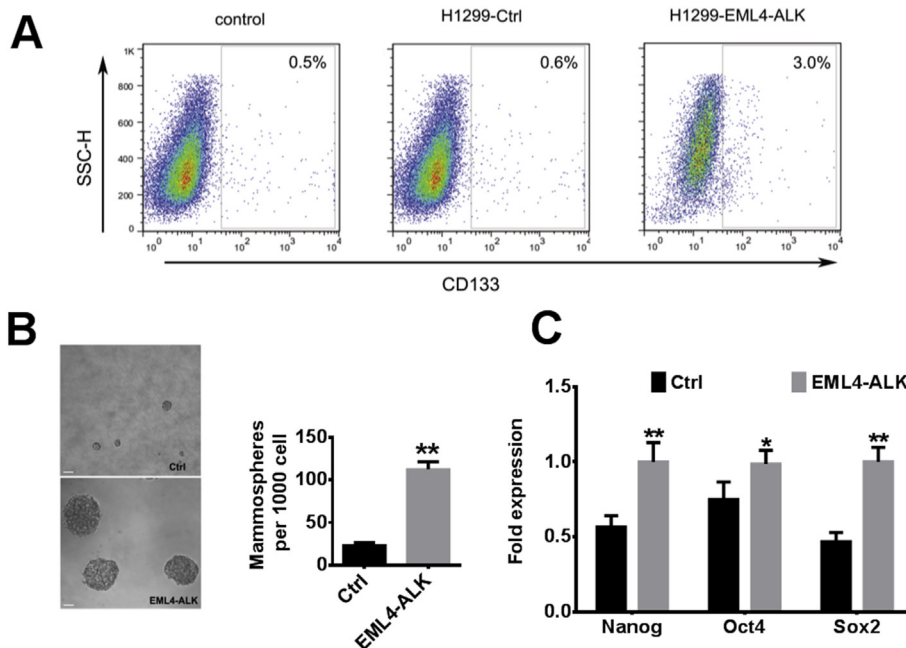


**Fig. 3.** H1299-EML4-ALK acquire cancer stem cell properties. (A) Flow cytometry detection of CD133 in H1299-Ctrl and H1299-EML4-ALK cells. (B) Mammosphere form of H1299-Ctrl and H1299-EML4-ALK cells. \*\*P < 0.01. Scale bars: 50  $\mu$ m. (C) Quantitative RT-PCR was used to quantify Nanog, Oct3/4 and Sox2 in H1299-Ctrl and H1299-EML4-ALK. \*P < 0.05; \*\*P < 0.01.

a concentration of 10  $\mu$ mol/L, resulted increased expression of E-cadherin. We also demonstrated that the specific inhibitor S3I-201, which resulted in marked inhibition of STAT3 phosphorylation at a concentration of 20  $\mu$ mol/L, do no affect the expression of E-cadherin. Meanwhile, we treated H1299 cells expressing EML4-ALK

with cirizotinib (10 nmol/L) as positive control (Fig. 4D). We further confirmed the role of ERK1/2 in EML4-ALK induced EMT by wound-healing assay and found that inhibition of ERK1/2 phosphorylation resulted in a markedly decrease in cell migration (Fig. 4C). Taken together, our observation indicated that ERK

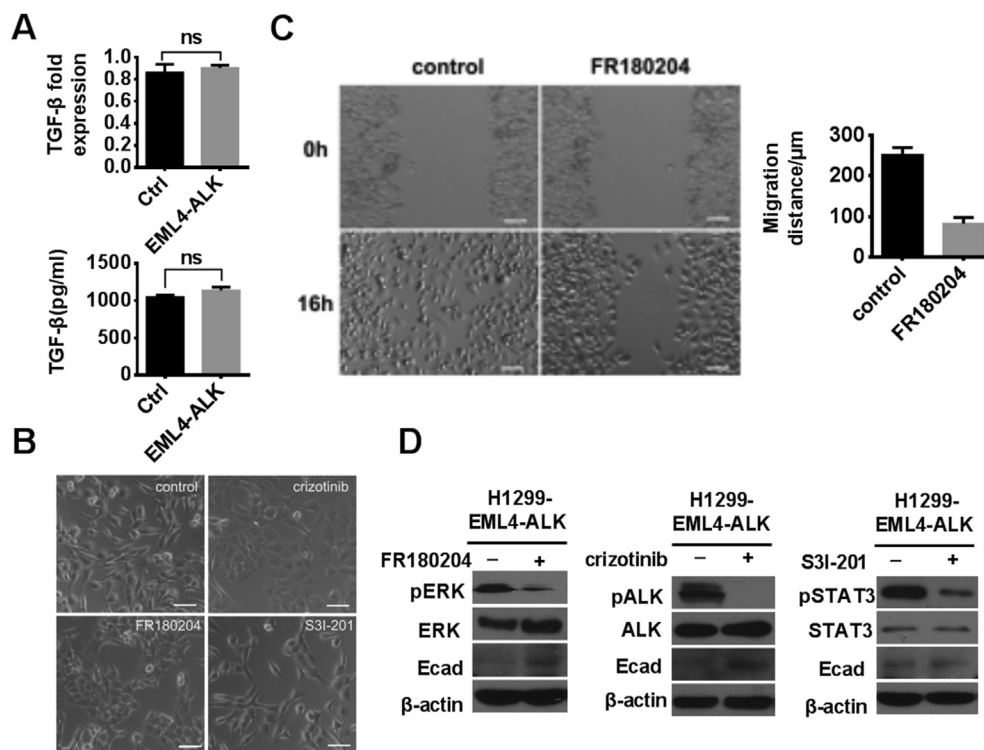


**Fig. 4.** ERK1/2 inhibition reverse EMT in H1299-EML4-ALK cells. (A) mRNA expression and secretion of TGF- $\beta$ 1 detected by quantitative real-time PCR and elisa, respectively. (B) Morphology of H1299-EML4-ALK cells treated with FR180204 (10  $\mu$ M), crizotinib (10 nM) and S3I-201(20  $\mu$ M) for 24 h. Scale bars: 50  $\mu$ m. (C) H1299-EML4-ALK cells were treated with FR180204 (10  $\mu$ M), crizotinib (10 nM) and S3I-201(20  $\mu$ M) for 24 h, cell extracts were analyzed by immunoblotting. (D) Motility of H1299-EML4-ALK cells treated with FR180204 or not, measured by wound-healing assay. \*\*P < 0.01. Scale bars: 100  $\mu$ m.

signaling pathway plays an key role in EML4-ALK induced EMT in H1299 cells.

#### 4. Discussion

Clinicopathological studies have showed that EML4-ALK translocations tends to occur in patients with more advanced NSCLC and manifest an aggressive clinical course [4,14]. In this study, we demonstrated that H1299-EML4-ALK cells display an EMT phenotype, which was characterized by acquiring spindle-like morphology, down-regulating the expression of E-cadherin with a concomitant increase of fibronectin, and enhancing migratory and invasive potential. Similarly to our findings, previous study have found that expression of NPM-ALK, the most thoroughly studied ALK-fusion protein, induce a typical transformed phenotype with spindle-shaped cell morphology and increase cell migration [15]. Colomba et al. has further indicated that ALK regulates the activity of Rho family GTPases, which resulted in RAC1 activation, thus increasing migration and invasion. The results of our study not only show that EML4-ALK activity modulate cytoskeletal rearrangements to enhance cell migration and invasion in H1299 NSCLC cells, but also we demonstrate that EML4-ALK increased expression of EMT-inducing transcription factors, snail and slug, which suggests cells undergoing epithelial–mesenchymal transition.

Compelling evidence relating EMT to the emergence of a CSC-like phenotype. The Weinberg group reported that EMT induced in mammary epithelial cells by TGF- $\beta$ 1, Twist or snail, leads to the evolution of the CD44<sup>high</sup>/CD24<sup>low</sup> population which shows an stem cell-like characteristics with increased ability to form mammospheres, soft agar colonies and tumors [11]. Considered to the study in NSCLC cell lines and fresh lung tumor tissues which suggest CD133<sup>+</sup> as a lung CSC marker [16], it is of interest that H1299-EML4-ALK NSCLC cell lines displayed a significant increased numbers of CD133<sup>+</sup> cells, relative to that of H1299-Ctrl cells. Evidence that subpopulations of cells within H1299-EML4-ALK cells display characteristics of cancer stem cells is further supported in our study using a panel of cancer stem cell markers and sphere formation. These observations suggest that, EML4-ALK confers subpopulations of NSCLC cells with cancer stem cell traits.

Members of the transforming growth factor- $\beta$  (TGF- $\beta$ ) family have been implicated as the main and best characterized inducers of EMT and show a role for TGF- $\beta$  in regulating breast cancer stem cell phenotypes [17,18]. In addition, increased secretion and expression of TGF- $\beta$ 1 was found in crizotinib resistant H2228 cells harboring EML4-ALK translocation, which undergo EMT [19]. However, our results detected no significantly difference in secretion and expression of TGF- $\beta$ 1 between H1299-EML4-ALK cells and H1299-Ctrl cells. Receptor tyrosine kinase activated signaling pathways, including Ras, MAP kinase, PI3 kinase, STAT3 and Rac/Cdc42, are also clearly involved in EMT [20–22]. A recent study reported that ERK1/2 signaling plays a key role in governing the mesenchymal character of NSCLC cells and inhibition of ERK1/2 prevents EMT in lung cancer cells [23]. Based on these findings, we assessed the effect of ERK1/2 on promoting EMT in H1299-EML4-ALK cells. Our study showed that blockage of ERK1/2 by FR180204, a selective ERK inhibitor, antagonizes down-regulation of E-cadherin and cell migration induced by EML4-ALK, whereas inhibition of STAT3 by S31-201 do not have this effect. These results suggested that EML4-ALK promote mesenchymal phenotypes through the MAPK pathway in H1299 NSCLC cells.

In summary, our results show that H1299 NSCLC cells expressing EML4-ALK acquire EMT features with increased migration and invasion. In addition, we demonstrate that activation of ERK signaling pathway is involved in Epithelial–Mesenchymal

Transition of H1299- EML4-ALK cells. In the future, therefore, inhibition of ERK signaling pathway could be an potential strategy in treatment of NSCLC patients with EML4-ALK translocation.

#### Conflict of interest

The authors have declared that no conflict of interest exists.

#### Acknowledgments

We thank Yong-sheng Wang, Ph.D. for valuable suggestion for this paper. We thank Dr Hiroyuki Mano (Jichi Medical University, Japan) for the kind gift of EML4-ALK plasmid. This work was financially supported by the National Natural Sciences Foundation of China (Proj. No. H1615).

#### Transparency document

Transparency document related to this article can be found online at <http://dx.doi.org/10.1016/j.bbrc.2015.02.114>.

#### References

- [1] M. Soda, Y.L. Choi, M. Enomoto, S. Takada, Y. Yamashita, S. Ishikawa, S.-i. Fujiwara, H. Watanabe, K. Kurashina, H. Hatanaka, M. Bando, S. Ohno, Y. Ishikawa, H. Aburatani, T. Niki, Y. Sohara, Y. Sugiyama, H. Mano, Identification of the transforming EML4-ALK fusion gene in non-small-cell lung cancer, *Nature* 448 (2007) 561–566.
- [2] T. Sasaki, S.J. Rodig, L.R. Chirieac, P.A. Jänne, The biology and treatment of EML4-ALK non-small cell lung cancer, *Eur. J. Cancer* 46 (2010) 1773–1780.
- [3] K. Inamura, K. Takeuchi, Y. Togashi, S. Hatano, H. Ninomiya, N. Motoi, M.-y. Mun, Y. Sakao, S. Okumura, K. Nakagawa, M. Soda, Y. Lim Choi, H. Mano, Y. Ishikawa, EML4-ALK lung cancers are characterized by rare other mutations, a TTF-1 cell lineage, an acinar histology, and young onset, *Mod. Pathol.* 22 (2009) 508–515.
- [4] D.W.-S. Wong, E.L.-H. Leung, K.K.-T. So, I.Y.-S. Tam, A.D.-L. Sihoe, L.-C. Cheng, K.-K. Ho, J.S.-K. Au, L.-P. Chung, M. Pik Wong, University of Hong Kong Lung Cancer Study Group, The EML4-ALK fusion gene is involved in various histologic types of lung cancers from nonsmokers with wild-type EGFR and KRAS, *Cancer* 115 (2009) 1723–1733.
- [5] E.L. Kwak, Y.-J. Bang, D.R. Camidge, A.T. Shaw, B. Solomon, R.G. Maki, S.-H.I. Ou, B.J. Dezube, P.A. Jänne, D.B. Costa, M. Varela-Garcia, W.-H. Kim, T.J. Lynch, P. Fidias, H. Stubbs, J.A. Engelman, L.V. Sequist, W. Tan, L. Gandhi, M. Mino-Kenudson, G.C. Wei, S.M. Shreeve, M.J. Ratain, J. Settleman, J.G. Christensen, D.A. Haber, K. Wilner, R. Salgia, G.I. Shapiro, J.W. Clark, A.J. Iafrate, Anaplastic lymphoma kinase inhibition in non-small-cell lung cancer, *N. Engl. J. Med.* 363 (2010) 1693–1703.
- [6] Y.L. Choi, M. Soda, Y. Yamashita, T. Ueno, J. Takashima, T. Nakajima, Y. Yatabe, K. Takeuchi, T. Hamada, H. Haruta, Y. Ishikawa, H. Kimura, T. Mitsudomi, Y. Tanio, H. Mano, EML4-ALK mutations in lung cancer that confer resistance to ALK inhibitors, *N. Engl. J. Med.* 363 (2010) 1734–1739.
- [7] Y. Nakaya, G. Sheng, EMT in developmental morphogenesis, *Cancer Lett.* 341: 9–15.
- [8] K. Vleminckx, L. Vakaet Jr., M. Mareel, W. Fiers, F. Van Roy, Genetic manipulation of E-cadherin expression by epithelial tumor cells reveals an invasion suppressor role, *Cell* 66 (1991) 107–119.
- [9] J.P. Thiery, J.P. Sleeman, Complex networks orchestrate epithelial-mesenchymal transitions, *Nat. Rev. Mol. Cell. Biol.* 7 (2006) 131–142.
- [10] A. Barrallo-Gimeno, M.A. Nieto, The Snail genes as inducers of cell movement and survival: implications in development and cancer, *Development* 132 (2005) 3151–3161.
- [11] S.A. Mani, W. Guo, M.-J. Liao, E.N. Eaton, A. Ayyanan, A.Y. Zhou, M. Brooks, F. Reinhard, C.C. Zhang, M. Shiptsin, L.L. Campbell, K. Polyak, C. Briskin, J. Yang, R.A. Weinberg, The epithelial-mesenchymal transition generates cells with properties of stem cells, *Cell* 133 (2008) 704–715.
- [12] S.-H. Chiou, M.-L. Wang, Y.-T. Chou, C.-J. Chen, C.-F. Hong, W.-J. Hsieh, H.-T. Chang, Y.-S. Chen, T.-W. Lin, H.-S. Hsu, C.-W. Wu, Coexpression of Oct4 and nanog enhances malignancy in lung adenocarcinoma by inducing cancer stem cell-like properties and Epithelial–Mesenchymal transdifferentiation, *Cancer Res.* 70 (2010) 10433–10444.
- [13] A.T. Shaw, P.P. Hsu, M.M. Awad, J.A. Engelman, Tyrosine kinase gene rearrangements in epithelial malignancies, *Nat. Rev. Cancer* 13 (2013) 772–787.
- [14] M. Takeda, I. Okamoto, K. Sakai, H. Kawakami, K. Nishio, K. Nakagawa, Clinical outcome for EML4-ALK-positive patients with advanced non-small-cell lung cancer treated with first-line platinum-based chemotherapy, *Ann. Oncol.* 23 (2012) 2931–2936.
- [15] C. Ambrogio, A.D. Voena C Fau - Manazza, R. Manazza Ad Fau - Piva, L. Piva R Fau - Riera, L. Riera L Fau - Barberis, C. Barberis L Fau - Costa, G. Costa C Fau -

- Tarone, P. Tarone G Fau - Defilippi, E. Defilippi P Fau - Hirsch, E. Hirsch E Fau - Boeri Erba, S. Boeri Erba E Fau - Mohammed, O.N. Mohammed S Fau - Jensen, G. Jensen On Fau - Palestro, G. Palestro G Fau - Inghirami, R. Inghirami G Fau - Chiarle, R. Chiarle, p130Cas mediates the transforming properties of the anaplastic lymphoma kinase.
- [16] A. Eramo, F. Lotti, G. Sette, E. Pilozzi, M. Biffoni, A. Di Virgilio, C. Conticello, L. Ruco, C. Peschle, R. De Maria, Identification and expansion of the tumorigenic lung cancer stem cell population, *Cell. Death Differ.* 15 (2007) 504–514.
- [17] J. Yang, R.A. Weinberg, Epithelial-mesenchymal transition: at the crossroads of development and tumor metastasis, *Dev. Cell.* 14 (2008) 818–829.
- [18] A.-P. Morel, M. Lièvre, C. Thomas, G. Hinkal, S. Ansieau, A. Puisieux, Generation of breast cancer stem cells through epithelial-mesenchymal transition, *PLoS ONE* 3 (2008) e2888.
- [19] H.R. Kim, W.S. Kim, Y.J. Choi, C.M. Choi, Jin K. Rho, J.C. Lee, Epithelial-mesenchymal transition leads to crizotinib resistance in H2228 lung cancer cells with EML4-ALK translocation, *Mol. Oncol.* 7 1093–1102.
- [20] B. Boyer, S. Roche, M. Denoyelle, J. Paul Thiery, Src and Ras are involved in separate pathways in epithelial cell scattering, 1997.
- [21] W. Birchmeier, V. Brinkmann, C. Niemann, S. Meiners, S. DiCesare, H. Naundorf, M. Sachs, Role of HGF/SF and C-Met in Morphogenesis and Metastasis of Epithelial Cells, *Ciba Foundation Symposium 212-Plasminogen-Related Growth Factors*, John Wiley & Sons, Ltd, 2007, pp. 230–251.
- [22] H. Xiong, J. Hong, W. Du, Y.-w. Lin, L.-l. Ren, Y.-c. Wang, W.-y. Su, J.-l. Wang, Y. Cui, Z.-h. Wang, J.-Y. Fang, Roles of STAT3 and ZEB1 proteins in e-cadherin down-regulation and human colorectal cancer epithelial-mesenchymal transition, *J. Biological Chem.* 287 (2012) 5819–5832.
- [23] J.M. Buonato, M.J. Lazzara, ERK1/2 blockade prevents epithelial–mesenchymal transition in lung cancer cells and promotes their Sensitivity to EGFR inhibition, *Cancer Res.* 74 (2014) 309–319.